Available online at www.sciencedirect.com
SCIENCE DIRECT®
International Journal of Heat and Mass Transfer 48 (2005) 1107–1116
International Journal of HEAT and MASS TRANSFER
www.elsevier.com/locate/ijhmt

Heat transfer properties of nanoparticle-in-fluid dispersions (nanofluids) in laminar flow

Ying Yang [a], Z. George Zhang [b,*], Eric A. Grulke [a,*], William B. Anderson [b], Gefei Wu [b]

[a] Department of Chemical and Materials Engineering, University of Kentucky, Lexington, KY 40506, USA
[b] New Product Development Laboratory, The Valvoline Company, P.O. Box 14000, Lexington, KY 40509, USA

Received 12 February 2004; received in revised form 15 September 2004
Available online 10 December 2004

Abstract

The convective heat transfer coefficients of several nanoparticle-in-liquid dispersions (nanofluids) have been measured under laminar flow in a horizontal tube heat exchanger. The nanoparticles used in this research were graphitic in nature, with aspect ratios significantly different from one ($l/d \approx 0.02$). The graphite nanoparticles increased the static thermal conductivities of the fluid significantly at low weight fraction loadings. However, the experimental heat transfer coefficients showed lower increases than predicted by either the conventional heat transfer correlations for homogeneous fluids, or the correlations developed from the particle suspensions with aspect ratios close to one. New correlations on heat transfer need to be developed for nanofluid systems.

Keywords: Nanoparticles; Dispersions; Thermal conductivity; Heat transfer coefficient; Laminar flow

1. Introduction

Heat transfer fluids provide an environment for adding or removing energy to systems, and their efficacies depend on their physical properties, such as thermal conductivity, viscosity, density, and heat capacity. Low thermal conductivity is often the primary limitation for heat transfer fluids. Recently, there has been interest in using nanoparticles as additives to modify heat transfer fluids to improve their performance [1–12]. Dispersion or suspension of nanoparticles of high thermal conductivities in heat transfer fluids (the so-called "nanofluids") is one of the methods for improving the thermal conductivity of the mixtures [1–5], and thus increasing their heat transfer coefficient in various applications. Some examples of nanofluids with improved thermal conductivity include metal nanoparticle suspensions as working fluids in microchannel heat exchangers [1], copper oxide particles suspended in water [3], and silicon carbide nanoparticles in water or ethylene glycol [9,12]. Compared with millimeter- or micrometer-sized particle suspensions, nanofluids possess better long-term stability and rheological properties, and can have dramatically higher thermal conductivities. Current efforts have mainly been focused on low aspect ratio nanoparticle

* Corresponding authors. Tel.: +1 8593573510; fax: +1 8593573530 (Z.G. Zhang); tel.: +1 8592576097; fax: +1 8593234922 (E.A. Grulke).
E-mail addresses: zzhang@ashland.com (Z.G. Zhang), egrulke@engr.uky.edu (E.A. Grulke).

0017-9310/$ - see front matter © 2004 Elsevier Ltd. All rights reserved.
doi:10.1016/j.ijheatmasstransfer.2004.09.038

Nomenclature

A	area
C_P	heat capacity
d	diameter of particle
D	diameter of test tube
g	acceleration due to gravity
h	heat transfer coefficient
k	thermal conductivity
l	thickness of particle
L	length of test tube
$\dot{m}$	mass flow rate
n	shape factor
q	heat transfer rate
T	temperature
U	overall heat transfer coefficient
W	weight flow of fluid

Greek symbols

β	coefficient of expansion
μ	viscosity
v	kinematic viscosity
ρ	density
ϕ	volume fraction of nanoparticles
Gr	Grashoff number
Gz	Graetz number
Nu	Nusselt number
Pe	Peclet number
Pr	Prandtl number
Re	Reynolds number

Subscripts

b	bulk
e	equivalent
eff	effective
f	fluid
hf	heating fluid
i	inside
in	inlet
o	outside
out	outlet
p	particle
w	wall

dispersions (disks), since controlling the thickening effect of the high aspect ratio particles (rods) is still a very challenging task [10,13].

A model has long been established by Hamilton and Crosser [14] to estimate the effective thermal conductivity, k_{eff}, of macroscopic solid–liquid mixtures, which is given in the following equation:

$$\frac{k_{\text{eff}}}{k_{\text{f}}} = \frac{k_{\text{p}} + (n-1)k_{\text{f}} - (n-1)\phi(k_{\text{f}} - k_{\text{p}})}{k_{\text{p}} + (n-1)k_{\text{f}} + \phi(k_{\text{f}} - k_{\text{p}})} \tag{1}$$

in which k_{f} and k_{p} are the thermal conductivities of the fluid and particles, respectively. ϕ is the volume fraction of the particles, and n is the empirical shape factor. Large aspect ratio particles, such as carbon nanotubes [10], have high values of n in Eq. (1), and therefore more potential for thermal conductivity enhancement. However, the addition of large aspect ratio particles into a liquid may result in huge increase in viscosity as compared to the continuous phase [13].

Recent work by Choi and colleagues [4,5,8,10] indicates that the thermal conductivity increase caused by the addition of nanometer-sized particles is much higher than predicted by the above equation. For example, the addition of 0.3 vol% of copper nanoparticles increases the thermal conductivity of ethylene glycol by 40% [8], and 1 vol% carbon nanotubes lead to a 150% increase of the thermal conductivity of a synthetic poly(α-olefin) oil [10].

Keblinski et al. [15] explored the mechanisms of heat transfer in nanofluids, and proposed four possible reasons for the contribution of the nanometer-sized particles to the increase of the thermal conductivity of the system: Brownian motion of the particles, molecular-level layering of the liquid at the liquid/solid interface, the nature of the heat transport in the nanoparticles, and the effects of nanoparticle clustering. The authors of the current communication believe there may be a synergistic effect of several above-mentioned mechanisms, among which the percolation effect may be favored for particles with high or low aspect ratios.

Nanofluids are multicomponent systems, and the morphology and orientation of the dispersed solids is complex. That is probably the reason that very few correlations have been developed for their convection heat transfer coefficients [16,17]. Considering the small size and the low volume fraction of the particles in most nanofluids, it might be reasonable to treat nanofluids as pure liquids in certain cases. Under these circumstances, the conventional correlations for homogeneous liquids might be applied to these systems. Three such correlations are the Seider–Tate equation for convective heat transfer of laminar flow in tubes [18], the Oliver correlation [19], and the Eubank and Proctor correlation [20].

The Seider–Tate equation is [18]

$$Nu = 1.86 Re^{1/3} Pr^{1/3} \left(\frac{D}{L}\right)^{1/3} \left(\frac{\mu_{\text{b}}}{\mu_{\text{w}}}\right)^{0.14} \tag{2}$$

in which Nu is the Nusselt number, Re is the Reynolds number, and Pr is the Prandtl number. $(\frac{\mu_{\text{b}}}{\mu_{\text{w}}})^{0.14}$ repre-

sents the radial variation of fluid properties and natural convection effect.

The Oliver correlation [19] for horizontal flow in tubes is

$$Nu\left(\frac{\mu_w}{\mu_b}\right)^{0.14} = 1.75(Gz + 5.6\times10^{-4}(Gr\cdot Pr\cdot L/D)^{0.70})^{1/3} \quad (3)$$

in which Gz is the Graetz number, $Gz = \frac{WC_p}{kL}$, Gr is the Grashoff number, $Gr = \frac{\beta_f \Delta T D^3 \rho_f^2 g}{\mu_f^2}$, W is weight flow of fluid, and β_f, ρ_f, and μ_f are the coefficients of expansion, the density, and the viscosity of fluid measured at film temperature, respectively.

The Eubank and Proctor correlation [20] for laminar flow in horizontal tubes is

$$Nu\left(\frac{\mu_w}{\mu_b}\right)^{0.14} = 1.75(Gz + 12.6(Gr\cdot Pr\cdot D/L)^{0.40})^{1/3} \quad (4)$$

In both Eqs. (3) and (4) the Grashoff number, Prandtl number, and the ratio of L/D are intended to account for the effect of the natural convection.

Only a few papers have discussed the heat transfer coefficients of nanofluids in convective flows [1,6,7,16,17]. Choi [1] pointed out that heat transfer coefficients should increase with flow rates or with increasing thermal conductivities of the fluid provided that other properties of the nanofluid system, such as heat capacity, density, and viscosity, are kept the same as the base fluid. If a nanofluid can have high thermal conductivity at low volume fractions, a high heat transfer coefficient might be obtainable without the pumping power being increased significantly. In heat exchanger design, the length of the exchange surface affects the local heat transfer coefficient via entrance effects and other factors. In some cases, using nanofluids can help achieve higher exchanger efficiency without increasing exchanger size. Recently Li and Xuan [16,17] studied convective heat transfer and flow characteristics of Cu-water nanofluids. The heat transfer coefficients of their nanoparticle suspensions are much higher than that of the base fluid and, when the volume fraction of nanoparticles is low, the friction factor of the fluids is not changed. They gave the new correlation for the convection heat transfer coefficient of nanofluids in a horizontal tube as [17]:

$$Nu = 0.4328(1.0 + 11.285\phi^{0.754}Pe^{0.218})Re^{0.333}Pr^{0.4} \quad (5)$$

in which Pe is the particle Peclet number.

The purpose of this article is to relate increases of thermal conductivity with the increases of the heat transfer coefficient for nanofluids containing low aspect ratio nanoparticles. The data are compared to Eqs. (2)–(5) to determine whether the correlations developed for homogenous fluids could be applied to the nanoparticle dispersions with aspect ratios different from one.

2. Experimental

Two series of nanofluids are investigated in this study with different base fluids. The base fluid for Series 1 (abbreviated as BF#1 hereafter) is a commercial automatic transmission fluid (ATF), while that for Series 2 (abbreviated as BF#2 hereafter) is a mixture of two commonly used synthetic baseoils with commercial additive packages. The experimental nanofluids listed in Table 1 are stable dispersions of base fluids with nanoparticles (they show no signs of settling after 30 days of rest).

All fluids were tested at two different temperatures. Comparing fluid EF#1-1 and EF#1-2 illustrates the effects of nanoparticles loading. Comparing fluid EF#1-1 with EF#2-2 illustrates the effects of base fluid differences. Comparing fluid EF#2-1 with EF#2-2 illustrates the effects of different nanoparticles sources. The average diameter of the graphite nanoparticle is about 1–2 μm, with the thickness around 20–40 nm ($l/d = 0.02$).

The following physical properties of the nanofluids were measured: thermal conductivity (k), density (ρ), heat capacity (C_P) and kinematic viscosity (v). Thermal conductivity measurements were done by using an in-house transient hot-wire device based on the design by Nagasaka and Nagashima [21]. Density was measured using a pycnometer. Heat capacity was measured using a differential scanning calorimetry (TA Instruments, Model 2920 Modulated). Kinematic viscosity was measured using a reverse tube capillary viscometer.

A small volume (~100 ml) flow loop heat transfer system has been constructed in-house. A schematic is presented in Fig. 1, with the geometry of the heat transfer sections illustrated. Because $L/D \gg 1$, it is reasonable to neglect the entrance effects in the test system. The whole system is heavily insulated to reduce heat loss. Pipes are wrapped with insulation material, and plastic fittings are attached at both ends of the test area to thermally isolate the connection. Static mixers are put at the ends of the test section to mix the fluids and improve accuracy of the bulk fluid temperature measurement. A positive displacement pump is used to control the fluid flow rate, and its displacement settings are calibrated to determine the volumetric flows (62–507 cm^3/min) that give average linear velocities between 6.3 and

Table 1
Experimental fluids

	Base fluid	Nanoparticle	Particle loading
EF#1-1	BF#1	Graphite	2 wt%
EF#1-2	BF#1	Graphite	2.5 wt%
EF#2-1	BF#2	Graphite[a]	2 wt%
EF#2-2	BF#2	Graphite	2 wt%

[a] From a different source than that used in the other experimental fluids.

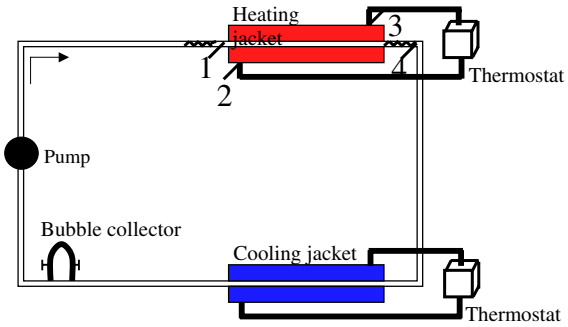

	Length (cm)	Inside diameter (cm)	Outside diameter (cm)	Roughness
Test tube	45.7	0.457	0.635	smooth
Heating jacket	45.7	1.09	/	smooth

Fig. 1. Heat transfer testing apparatus. (/) thermocouple.

52 cm/s. The fluid first passes through the thermostatic counter-current flow heating jacket in which water is used as the heating fluid, with its temperature set at either 50 °C or 70 °C. Four thermocouples are placed as shown in Fig. 1, two of which, 1 and 4, measure the fluid temperature at the inlet and outlet of the test area, and the other two, 2 and 3, are placed at the outlet and inlet of the heating jacket to measure water temperature. A thermostatic cooling jacket system, which is adjusted to 5 °C, is applied to the system for it to reach a steady state. The bubble collector collects and separates air bubbles from the fluid.

The experimental procedures are as follows: (1) the system is warmed up by starting the pump and heater. It takes 5–10 min to increase the temperature to the operating range and remove interior bubbles; (2) The flow rate is set, then open the cooling system for temperature control; (3) The system usually reaches a thermal steady state within 30 min (the variability of temperature measurements is ±0.1 °C): (4) Each measurement was repeated at least once. Average heat transfer coefficients were calculated. The deviations of the data are less than 2% in most cases and less than 5% in some high-flow rate cases.

3. Results and discussion

3.1. Physical properties of the test fluids

Physical properties of the base fluids and nanofluids are illustrated in Table 2. Thermal conductivities of the base fluids are typical for hydrocarbon fluids, in the range from 0.12 to 0.18 W/m K. The increase of the thermal conductivity of the nanofluid versus the base fluid ranges from 3% to 56%. If we apply Eq. (1) to the nanofluid with highest particle loading, EF#1-2, and assume that the thermal conductivity of the particle is 100 W/m K, and the empirical shape factor can be calculated from the size and shape of the particles, we would get a increase of at most 12.5%, much lower than the measured value, 56%. As being discussed earlier, Eq. (1) is deduced from suspensions containing millimeter to micrometer-sized particles, not nanometer-sized ones.

Density and heat capacity do not show much change as compared to those of the corresponding base fluid, which is reasonable due to the low volume fraction of the particles and moderate temperature change of the system. Kinematic viscosity is measured at four temperatures, 35, 43, 50 and 70 °C, in which the latter two are

Table 2
Physical properties of the test fluids

	Thermal conductivity		Density (g/cm^3)		Heat capacity (J/g K)	Kinematic viscosity (cSt)			
	k (W/m K)	k/k_0	35 °C	43 °C		35 °C	43 °C	50 °C	70 °C
BF#1	0.134	1	0.840	0.835	2.10	44.8	33.9	26.8	14.5
EF#1-1	0.173	1.29	0.847	0.842	2.10	41.4	30.6	23.7	12.2
EF#1-2	0.209	1.56	0.847	0.843	2.10	52.4	38.4	29.6	14.9
BF#2	0.148	1	0.820	0.815	2.20	28.5	21.9	17.5	9.78
EF#2-1	0.153	1.03	0.823	0.819	2.20	29.3	22.7	18.4	10.5
EF#2-2	0.182	1.23	0.825	0.820	2.20	31.1	24.1	19.5	11.2

the temperature of the heating fluid (water), and the first two are the calculated average temperature of the test fluid at the center of the test section at the corresponding heating fluid temperature. The dependence of kinematic viscosity on temperature is fairly significant for all fluids. Both base fluids were formulated with viscosity modifiers to get their viscosity to the appropriate range required by the application. Nanoparticles themselves modify fluid viscosity, so viscosity modifiers were adjusted to make sure they have similar viscosity with base fluids.

The heat transfer rate into the process fluid is

$$q = \dot{m}C_P(T_{\text{out}} - T_{\text{in}}) \tag{6}$$

The inlet and outlet temperature measurements are based on the average fluid temperature taken after the static mixers. The heat transfer rate from the heating fluid is

$$q_{\text{hf}} = \dot{m}_{\text{hf}}C_{\text{Phf}}(T_{\text{out}} - T_{\text{in}})_{\text{hf}} \tag{7}$$

Subscript hf is used to represent the heating fluid. The differences between energy lost by the heating fluid and energy gained by the process fluid were around 25%, which is typical for a small-scale testing equipment. The mass flow rate of the heating fluid is much higher than that of the test fluid so the value of the temperature difference, $(T_{\text{out}} - T_{\text{in}})_{\text{hf}}$, is very small (less than 1 °C) and contributes to the energy balance inaccuracies. Incomplete isolation could also contribute to energy losses in the system. The heat obtained by the process fluid was used as the energy transferred as it was the more accurate value.

We can calculate the heat transfer coefficient of the test fluid, h_i, through the following equation:

$$\frac{1}{U} = \frac{1}{h_i(A_i/A_o)} + \frac{D_o}{2k}\ln\frac{D_o}{D_i} + \frac{1}{h_o} \tag{8}$$

where U is the overall heat transfer coefficient, k is the thermal conductivity of the tube wall, and h_i and h_o are the individual heat transfer coefficients of the inside and outside fluids, respectively. U is given by

$$U = \frac{q}{A_o\Delta T} \tag{9}$$

where $A_o = \pi D_o L$, and ΔT is the log-mean temperature difference.

The outside heat transfer coefficient h_o is computed from the Monrad and Pelton's equation [22] for turbulent flow in annuli, $Nu = 0.020Re^{0.8}Pr^{1/3}(D_2/D_1)^{0.53}$, in which D_1 and D_2 are the inner and outer diameter of the annulus respectively. The heating fluid is water in turbulent flow, so the heat transfer coefficients (3780 W/m^{2}K for 50 °C and 4784 W/m^{2}K for 70 °C) are much higher than that of the process fluid. The equivalent diameter is used for heat transfer calculations, $D_e = \frac{ID_a^2 - OD^2}{OD}$, where ID_a is the inside diameter of the annulus and OD is the outside diameter of the tube.

The thermal conductivity of base fluid #1 (BF#1) is 0.134 W/m K, and its viscosity decreases by a factor of 3 over the temperature range 35–70 °C. Figs. 2 and 3 show the heat transfer data as a function of Reynolds number for all test fluids at different experimental conditions. These figures illustrate the effects of Reynolds number, temperature, nanoparticle loading and source, and base fluid, on the heat transfer properties of nanofluids. A power law correlation, $h = a \cdot Re^b$, has been used to represent the base fluid data as an aid to the eye, with R^2 values as 0.97 for BF#1 and 0.95 for BF#2, respectively.

3.1.1. Reynolds number effect

The experiments were conducted over a range of Reynolds numbers, $5 < Re < 110$. The base fluids and the nanofluids all show increasing heat transfer coefficients as the average flow velocity, and Reynolds numbers increase (Figs. 2 and 3).

3.1.2. Nanoparticle loading effect

The effects of nanoparticle loading can be seen by comparing EF#1-1 with EF#1-2 (Fig. 2a and b). EF#1-1 with 2 wt% graphite nanoparticles has a heat

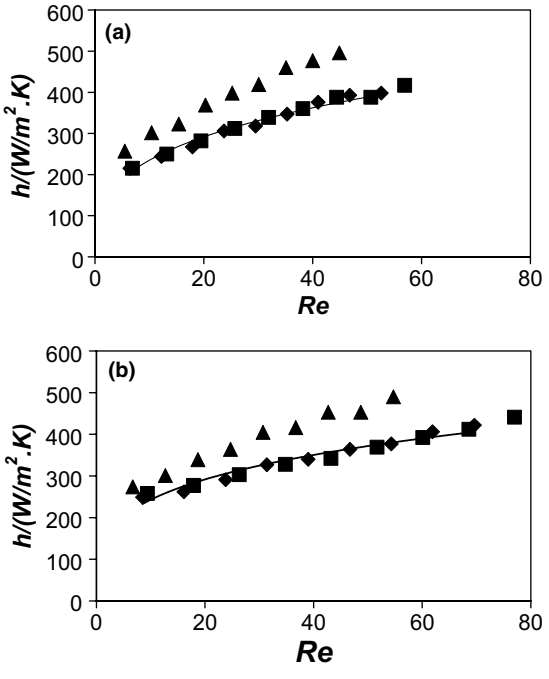

Fig. 2. Plot of heat transfer coefficient versus Reynolds number for Series 1 fluids (a) 50 °C, (b) 70 °C. (♦) base fluid 1; (■) EF#1-1; (▲) EF#1-2; (—) fitting for BF#1 according to power law correlation.

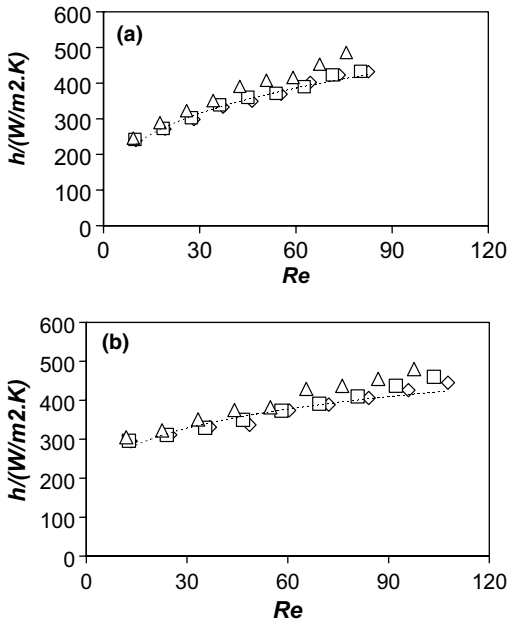

Fig. 3. Plot of heat transfer coefficient versus Reynolds number for Series 2 fluids (a) 50 °C, (b) 70 °C. (◊) Base fluid 2; (□) EF#2-1; (△) EF#2-2; (----) fitting for BF#2 according to power law correlation.

transfer coefficient similar to that of the base fluid (BF#1) at both temperatures. There is a modest increase in the heat transfer coefficient, but it is not much different from the experimental error. At 50 °C, the nanofluid (EF#1-2) with the higher loading (2.5 wt%) has a typical increase in heat transfer coefficient of 22% over the base fluid, while its thermal conductivity is about 50% higher than that of the base fluid. At 70 °C, the heat transfer coefficient increase averages 15%.

The thermal conductivity ratios of the nanofluids to the base fluid are about 1.30 and 1.50, suggesting that under quiescent conditions, both nanofluids are above the percolation limit at which there is excellent particle-to-particle contact. However, the experimental results on heat transfer properties indicate that over the Reynolds number range, $5 < Re < 80$, the nanofluid with 2 wt% nanoparticles loading is not above the percolation limit, while the nanofluid with 2.5 wt% loading is.

3.1.3. Temperature effect

Fig. 2a shows that, at 50 °C, EF#1-2 has a typical increase in heat transfer coefficient of 22% over the base fluid. However, at 70 °C, the heat transfer coefficient increase averages only 15%. Several mechanisms may lead to smaller improvements in heat transfer coefficient between the nanofluids and the base fluids at higher temperature. These include: (1) rapid alignment of \nanoparticles in lower viscosity fluids, leading to less contact between nanoparticles, and (2) depletion of particles in the near-wall fluid phase [23], leading to an intrinsically lower thermal conductivity layer at the wall. Understanding and isolating which mechanism or mechanisms might be responsible for the experimental results will require significant future work, including computational fluid dynamic modeling of the flows in nanoparticle dispersions.

3.1.4. Nanoparticle source effect

Fig. 3a and b compare data for two different graphite nanoparticles at the same loading, 2 wt%, in base fluid 2. At 50 °C, the heat transfer coefficient of the base fluid is modeled well by the power law expression ($R^2 = 0.98$). The data for dispersion EF#2-1, which contains graphite particles from a different source than the rest of the nanofluids, suggests that this nanofluid is not above the percolation limit for this range of Reynolds numbers and temperatures. On the other hand, the fluid with graphite material used in the rest of the study, EF#2-2, shows increases in its heat transfer coefficient relative to that of the base fluid at higher Reynolds numbers ($Re > 40$). There may be similar effects such as nanoparticle alignment and nanoparticle separation near the wall that are sensitive to nanoparticle structure and interaction. The difference could be caused by particle shape, morphology, or surface treatment. In any case, this comparison demonstrates that one type of nanoparticle is more efficient than the other in increasing the heat transfer coefficient of the nanofluid.

3.1.5. Base fluid effect

The choice of the base fluid also affects the heat transfer coefficients of nanofluids. In EF#1-1 and EF#2-2, the same graphite nanoparticles were dispersed in the two base fluids at 2 wt%. EF#1-1 has similar heat transfer coefficients to BF#1 at both temperatures. EF#2-2 has higher heat transfer coefficients than BF#2, particularly at higher Reynolds numbers. These data demonstrate that Reynolds number, temperature, nanoparticle loading, nanoparticle source, and the choice of the base fluid can all affect the heat transfer coefficients of nanofluids.

3.2. Correlations for convective heat transfer

The correlations for the convective heat transfer of the single-phase fluid may be applied to predict h of a nanofluid system, if the volume fraction of particles is very low. Eq. (2) can be re-written into a form more convenient for identifying the impact of Reynolds number on the heat transfer coefficient:

$$\Omega = Nu \cdot Pr^{-1/3}\left(\frac{L}{D}\right)^{1/3}\left(\frac{\mu_b}{\mu_w}\right)^{-0.14} = 1.86Re^{1/3} \qquad (10)$$

Fig. 4 shows the experimental results plotted as Ω versus Re.

The 1/3-dependence as predicted by Eq. (10) is clearly shown in Fig. 4. However, at low Reynolds number, $Re < 30$, the data are more scattered. The larger error at low Reynolds number is likely due to the effect of natural convection. As a first approximation, Eq. (10) is adequate, but it obviously misses important information about the thermal properties of the nanoparticle suspension, particularly at low Reynolds numbers.

The data sets can be correlated using the following equation:

$$\Omega = aRe^b \tag{11}$$

The results listed in Table 3 show that the Reynolds number exponent, b, of the nanofluid is fairly close to that of the base fluid, with the value at 70 °C lower than that at 50 °C for the same fluid. This effect seems to be more apparent for the Series 2 fluids (i.e., BF#2, EF#2-1, and EF#2-2), and could be due to the fact that the viscosity of Series 1 fluids is higher. For fluids with higher viscosity, natural convection (for example, the term including the Grashoff number in Eq. (3)) contributes less to the heat transfer effect, which results in the smaller temperature dependence for the Series 1 fluids. The value of the pre-exponential coefficient, a, of the suspension is always lower than that of the corresponding base fluid. Fig. 5 shows that most of the experimental data for the nanofluids are below the theoretical line (Eq. (10)) while the base fluid values are generally the same as the theoretical line.

Eq. (10) provides a basis for comparing the heat transfer coefficients calculated from the theory with those calculated from the experimental data. Since density and heat capacity of the nanofluid are very close to those of the base fluid (Table 1), the heat transfer coefficient ratio should be sensitive to two important terms, $k^{2/3}$ and $(\frac{\mu_b}{\mu_w})^{-0.14}$. The comparison is listed in Table 4.

Table 4 indicates that the increase of the heat transfer coefficient of nanofluid is much less than that predicted from a conventional correlation. It seems that some

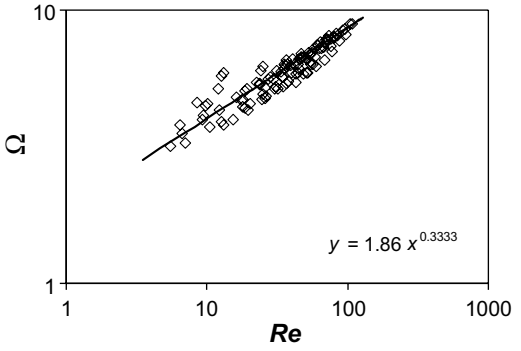

Fig. 4. Plot of Ω versus Reynolds number for all the test fluids. (◊) test data; (—) fitting according to Eq. (10).

Table 3
Coefficients of Eq. (11) for each test fluid

	Heat fluid temperature (°C)	a	b	R^2 of the fitting
BF#1	50	1.90 ± 0.13	0.33 ± 0.02	0.980
EF#1-1	50	1.64 ± 0.08	0.33 ± 0.01	0.991
EF#1-2	50	1.66 ± 0.10	0.34 ± 0.02	0.984
BF#1	70	2.28 ± 0.19	0.28 ± 0.02	0.964
EF#1-1	70	2.00 ± 0.19	0.28 ± 0.03	0.952
EF#1-2	70	1.88 ± 0.13	0.30 ± 0.02	0.976
BF#2	50	2.09 ± 0.14	0.31 ± 0.02	0.982
EF#2-1	50	2.17 ± 0.12	0.29 ± 0.01	0.985
EF#2-2	50	1.81 ± 0.13	0.33 ± 0.02	0.983
BF#2	70	3.11 ± 0.30	0.22 ± 0.02	0.931
EF#2-1	70	2.92 ± 0.30	0.23 ± 0.03	0.928
EF#2-2	70	2.66 ± 0.24	0.24 ± 0.02	0.948

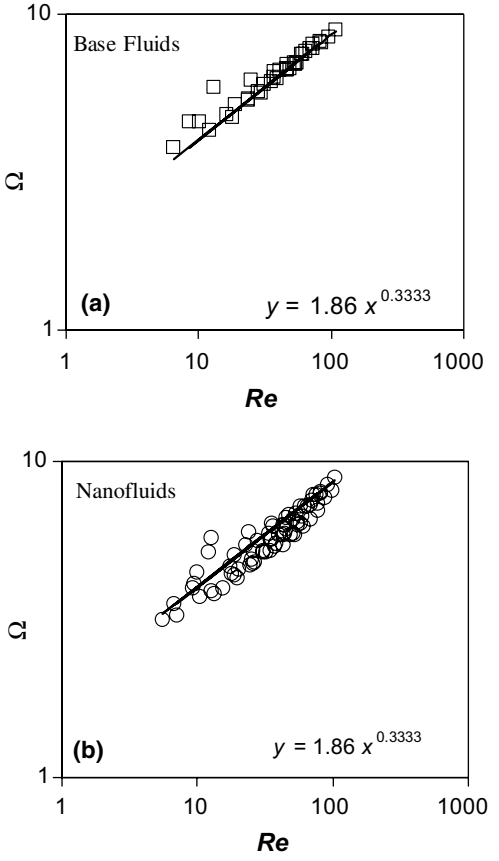

Fig. 5. Plot of Ω versus Reynolds number for base fluids and nanofluids. (□) test data on base fluids; (◯) test data on nanofluids; (—) fitting according to Eq. (10).

Table 4
Heat transfer coefficient ratios of nanofluid versus corresponding base fluid

	Heating fluid temperature (°C)	Eq. (10)	Experiment
$\frac{h(\text{EF}\#1\text{-}1)}{h(\text{BF}\#1)}$	50	1.19	1.03
	70	1.19	1.03
$\frac{h(\text{EF}\#1\text{-}2)}{h(\text{BF}\#1)}$	50	1.36	1.22
	70	1.36	1.15
$\frac{h(\text{EF}\#2\text{-}1)}{h(\text{BF}\#2)}$	50	1.02	1.01
	70	1.02	1.01
$\frac{h(\text{EF}\#2\text{-}2)}{h(\text{BF}\#2)}$	50	1.14	1.08
	70	1.14	1.07

special factors in the nanofluid mixture are affecting the heat transfer mechanisms, especially for Series 1 fluids at higher wall temperature. The results suggest that heat transfer property improvements can be made by varying the base fluid, the nanoparticle source, and the nanoparticle loading.

Nanoparticles may enhance the heat transfer coefficient by two mechanisms: an increase in the thermal conductivity of the overall system, and the movement of the nanoparticles relative to the streamlines. Higher temperature differentials between the process fluid and the heat source result in lower heat transfer coefficients than expected. As the process fluid begins to be heated at the entrance of the exchanger, the fluid viscosity decreases, the velocity profile ceases to be parabolic and

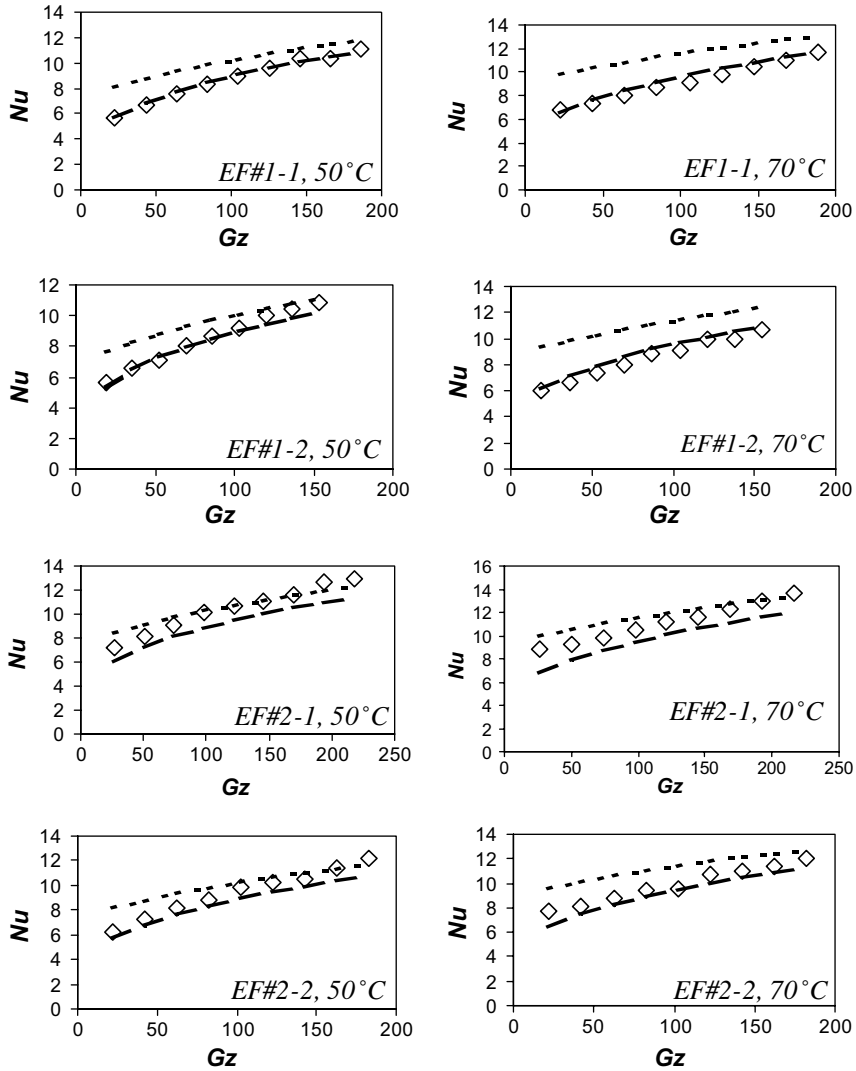

Fig. 6. Relationship between the Nusselt and Graetz numbers for the test fluids. (◊) test data; (----) calculation based on Oliver correlation [19]; (———) calculation based on Eubank and Proctor correlation [20].

starts to change. As shear rates change (the most change will occur near the wall), nanoparticles may align with the velocity. Alignment of the nanoparticles can decrease the thermal conductivities of fluids if the nanoparticle-nanoparticle interactions responsible for the enhanced heat transfer are disrupted. The shear force in the fluid or near the tube wall will make the particles orient to some extent, and break up the percolation structure. Higher shear rates can disperse nanoparticles that have "clustered", especially in a turbulent flow. However, in a laminar flow system, this dispersing effect might be relatively small. These experiments have a laminar flow ($5 < Re < 110$) with relatively high shear rate (between $100\,s^{-1}$ and $1000\,s^{-1}$), which may contribute to the lower heat transfer coefficients. Near wall particle depletion is another possible reason for the phenomenon. Moreover, adding particles into a fluid increases the viscosity of the final mixture, which may suppress the natural convection of the system. In summary, due to the possible mechanisms for nanoparticle movements in laminar flows under heating, Eq. (2) may not be directly applicable to the nanofluid system.

The correlation developed by Li and Xuan [16,17], Eq. (5), is based on a laminar flow of the nanofluids. However, this correlation predicts heat transfer coefficients that are much higher than the experimental values. The correlation developed by Li does not include the aspect ratio of the particles. Spherical copper nanoparticles were used in their work, while, in our system, the nanoparticles are disc-like graphite nanoparticles. There is at least one order of magnitude difference in the aspect ratio of the particles between these two cases.

The correlations by Oliver [19] and Eubank and Proctor [20] address natural convention that will occur in a laminar flow. The relationship between the Nusselt and Graetz numbers of the test fluids is plotted in Fig. 6, together with theoretical curves. It can be seen that the data from the Series 1 fluids fit the Oliver model fairly well, while the data from the Series 2 fluids lie in between the plots of these two models. This indicates that an improved correlation for heat transfer coefficient in nanofluid systems should be developed, which is the future direction of this research project.

4. Conclusion

The convection heat transfer performance of the graphite nanofluids were studied in laminar flow through a circular tube. The experimental results show that the nanoparticles increase the heat transfer coefficient of the fluid system in laminar flow, but the increase is much less than that predicted by current correlation based on static thermal conductivity measurements. The type of nanoparticles, particle loading, base fluid chemistry, and process temperature are all important factors to be considered while developing nanofluids for high heat transfer coefficients. Further investigation is needed to develop an appropriate heat transfer correlation for non-spherical nanoparticle dispersions.

Acknowledgments

The authors appreciate very much the continuous support and encouragement by Dr. Fran Lockwood of the Valvoline Company. ZGZ, WBA and GF would like to thank Dr. Steve Choi and Dr. Wenhua Yu of Argonne National Laboratory for the instructive discussion and tremendous help on the construction of the transient hot-wire rig and the heat transfer loop. The authors acknowledge the comments and suggestions of reviewers, who help improve the content of this paper.

References

[1] S.U.S. Choi, Enhancing thermal conductivity of fluid with nanoparticles, in: D.A. Siginer, H.P. Wang (Eds.), Development and Application of Non-Newronian Flows, The American Society of Mechanical Engineers, New York, NY, FED-vol. 231/MD-vol. 66, 1995, pp. 99–105.

[2] S. Lee, S.U.S. Choi, Application of metallic nanoparticle suspensions in advanced cooling systems, in: Y. Kwon, D. Davis, H. Chung (Eds.), Recent advances in solids/structures and application of metallic materials, The American Society of Mechanical Engineers, New York, NY, PVP-vol. 342/MD-vol. 72, 1996, pp. 227–234.

[3] J.A. Eastman, U.S. Choi, S. Li, L.J. Thompson, S. Lee, Enhanced thermal conductivity through the development of nanofluids, Materials Research Society Symposium Proceedings, vol. 457, Pittsburgh, PA, 1997, pp. 3–11.

[4] S. Lee, S.U.S. Choi, S. Li, J.A. Eastman, Measuring thermal conductivity of fluids containing oxide nanoparticles, J. Heat Transfer 121 (1999) 280–289.

[5] X. Wang, X. Xu, S.U.S. Choi, Thermal conductivity of nanoparticle-fluid mixture, J. Thermophys. Heat Transfer 13 (4) (1999) 474–480.

[6] Y. Xuan, Q. Li, Heat transfer enhancement of nanofluids, Int. J. Heat Transfer Fluid Flow 21 (2000) 58–64.

[7] Y. Xuan, W. Roetzel, Conceptions for heat transfer correlations of nanofluids, Int. J. Heat Mass Transfer 43 (2000) 3701–3707.

[8] J.A. Eastman, S.U.S. Choi, S. Li, W. Yu, L.J. Thompson, Anomalously increased effective thermal conductivities of ethylene glycol-based nanofluids containing copper nanoparticles, Appl. Phys. Lett. 78 (6) (2001) 718–720.

[9] H. Xie, J. Wang, T. Xi, Y. Liu, Thermal conductivity of suspensions containing nanosized SiC particles, Int. J. Thermophys. 23 (2) (2002) 571–580.

[10] S.U.S. Choi, Z.G. Zhang, W. Yu, F.E. Lockwood, E.A. Grulke, Anomalous thermal conductivity enhancement in nanotube suspensions, Appl. Phys. Lett. 79 (14) (2001) 2252–2254.

[11] H. Xie, J. Wang, T. Xi, Y. Liu, F. Ai, Q. Wu, Thermal conductivity enhancement of suspensions containing nanosized alumina particles, J. Appl. Phys. 91 (7) (2002) 4568–4572.

[12] H. Xie, J. Wang, T. Xi, Y. Liu, F. Ai, Thermal conductivity of suspensions containing SiC particles, J. Mater. Sci. Lett. 21 (2002) 193–195.
[13] J. Bicerano, J.F. Douglas, D.A. Brune, Model for the viscosity of particle dispersions, J. Macromol. Sci., Part C—Polym. Rev. 39 (4) (1999) 561–642.
[14] R.L. Hamilton, O.K. Crosser, Thermal conductivity of heterogeneous two-component system, IEC Fundam. 1 (1962) 182–191.
[15] P. Keblinski, S.R. Philpot, S.U.S. Choi, J.A. Eastman, Mechanisms of heat flow in suspensions of nano-sized particles (nanofluids), Int. J. Heat Mass Transfer 45 (2002) 855–863.
[16] Q. Li, Y. Xuan, Experimental investigation on convective heat transfer of nanofluids, Gongcheng Rewuli Xuebao (J. Eng. Thermophys.) 23 (6) (2002) 721–723.
[17] Q. Li, Y. Xuan, Convective heat transfer and flow characteristics of Cu-water nanofluid, Sci. China, Series E: Technol. Sci. 45 (4) (2002) 408–416.
[18] E.N. Sieder, G.E. Tate, Heat transfer and pressure drop of liquids in tubes, Ind. Eng. Chem. 28 (12) (1936) 1429–1435.
[19] D.R. Oliver, Effect of natural convection on viscous-flow heat transfer in horizontal tubes, Chem. Eng. Sci. 17 (1962) 335–350.
[20] C.C. Eubank, W.S. Proctor, Effect of natural convection on heat transfer with laminar flow in tubes, M.Sc. Thesis in Chemical Engineering, Massachusetts Institute of Technology, Cambridge, MA, 1951.
[21] Y. Nagasaka, A. Nagashima, Absolute measurement of the thermal conductivity of electrically conducting liquids by the transient hot-wire method, J. Phys. E: Sci. Instrum. 14 (1981) 1435–1440.
[22] C.C. Monrad, J.F. Pelton, Heat transfer by convection in annular spaces, Trans. Am. Inst. Chem. Eng. 38 (1942) 593–611.
[23] P.J.A. Hartman Kok, S.G. Kazarian, C.J. Lawrence, B.J. Briscoe, Near-wall particle depletion in a flowing colloidal suspension, J. Rheol. 46 (2) (2002) 481–493.